JACS
JOURNAL OF THE AMERICAN CHEMICAL SOCIETY

ARTICLE

pubs.acs.org/JACS

Lysine-Specific Molecular Tweezers Are Broad-Spectrum Inhibitors of Assembly and Toxicity of Amyloid Proteins

Sharmistha Sinha,[†] Dahabada H. J. Lopes,[†] Zhenming Du,[#] Eric S. Pang,[†,‡] Akila Shanmugam,[†] Aleksey Lomakin,[+] Peter Talbiersky,[¶] Annette Tennstaedt,[○] Kirsten McDaniel,[†] Reena Bakshi,[†] Pei-Yi Kuo,[†] Michael Ehrmann,[○] George B. Benedek,[⊗,+] Joseph A. Loo,[‡,§,⊥] Frank-Gerrit Klärner,[¶] Thomas Schrader,[¶] Chunyu Wang,[#] and Gal Bitan[*,†,∥,⊥]

[†]Department of Neurology, David Geffen School of Medicine, [‡]Department of Chemistry and Biochemistry, [§]Department of Biological Chemistry, [∥]Brain Research Institute, and [⊥]Molecular Biology Institute, University of California at Los Angeles, Los Angeles, California 90095, United States

[#]Department of Biology, Rensselaer Polytechnic Institute, Troy, New York 12180, United States

[¶]Institute of Organic Chemistry and [○]Center for Medical Biotechnology, University of Duisburg-Essen, 45117 Essen, Germany

[⊗]Department of Physics and [+]Materials Processing Center, Massachusetts Institute of Technology, Cambridge, Massachusetts 02139, United States

Supporting Information

ABSTRACT: Amyloidoses are diseases characterized by abnormal protein folding and self-assembly, for which no cure is available. Inhibition or modulation of abnormal protein self-assembly, therefore, is an attractive strategy for prevention and treatment of amyloidoses. We examined Lys-specific molecular tweezers and discovered a lead compound termed CLR01, which is capable of inhibiting the aggregation and toxicity of multiple amyloidogenic proteins by binding to Lys residues and disrupting hydrophobic and electrostatic interactions important for nucleation, oligomerization, and fibril elongation. Importantly, CLR01 shows no toxicity at concentrations substantially higher than those needed for inhibition. We used amyloid β-protein (Aβ) to further explore the binding site(s) of CLR01 and the impact of its binding on the assembly process. Mass spectrometry and solution-state NMR demonstrated binding of CLR01 to the Lys residues in Aβ at the earliest stages of assembly. The resulting complexes were indistinguishable in size and morphology from Aβ oligomers but were nontoxic and were not recognized by the oligomer-specific antibody A11. Thus, CLR01 binds already at the monomer stage and modulates the assembly reaction into formation of nontoxic structures. The data suggest that molecular tweezers are unique, process-specific inhibitors of aberrant protein aggregation and toxicity, which hold promise for developing disease-modifying therapy for amyloidoses.

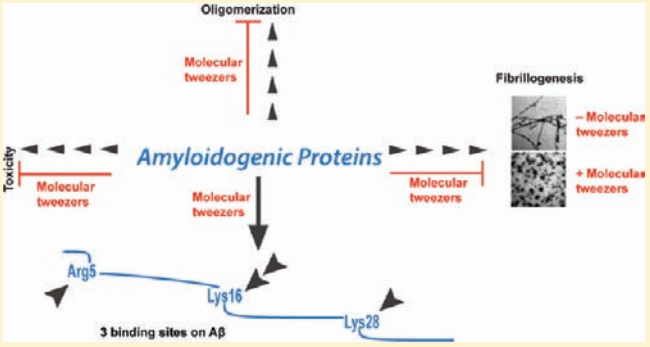

INTRODUCTION

Aberrant protein folding and aggregation cause over 30 human diseases.[1] For many of these diseases, there is no treatment at all, and in the best cases, the available therapy treats the symptoms but not the cause of the disease. Prominent examples of such diseases include Alzheimer's disease (AD), Parkinson's disease (PD), prion diseases, senile systemic amyloidosis (SSA), dialysis-related amyloidosis (DRA), and type-2 diabetes (T2D). In all of these diseases, one or more proteins that are part of normal physiology respond to genetic, environmental, or yet unknown stimuli by self-assembly into toxic oligomers and polymers.

The proteins involved can be structured or natively unstructured. Regardless of their physiologic structure or lack thereof, in disease conditions, these proteins self-associate abnormally, first into toxic oligomers and then to form amyloid fibrils.[2] Inhibition or modulation of these self-assembly processes, therefore, is an attractive strategy for prevention and treatment of amyloid-related diseases.[3]

Amyloid formation is a complex process that can proceed through many pathways. A common view of this process is as a nucleation-dependent polymerization reaction.[4−6] The nucleation step has high activation energy and therefore is the rate-limiting step, following which relatively rapid fibril elongation occurs. The molecular interactions controlling both nucleation and elongation include backbone hydrogen bonds complemented by

Received: July 10, 2011
Published: September 14, 2011

dx.doi.org/10.1021/ja206279b | J. Am. Chem. Soc. 2011, 133, 16958–16969

specific hydrophobic and electrostatic interactions involving side chains of particular amino acids.

We sought compounds that would interact with amyloidogenic proteins and disrupt their aberrant self-assembly, ideally at the earliest step in which monomers self-associate into small oligomers and/or nuclei. We reasoned that for effective perturbation of the oligomerization and aggregation processes, such compounds should interfere with as many types of molecular interactions as possible. We chose to focus on compounds that bind specifically to the amino acid Lys because Lys is unique in its ability to participate in both hydrophobic and electrostatic interactions.[7] In support of this rationale, Lys residues have been shown to play important roles in the assembly and toxicity of the proteins involved in AD and PD, amyloid β-protein (Aβ),[8−10] tau,[11−14] and α-synuclein.[15]

Lys-specific "molecular tweezers" (MTs) have been reported to bind to Lys with $K_d \approx 20\ \mu$M, with ~10-times lower affinity to Arg, and with little, if any, affinity to most other cationic biomolecules.[16] This unique selectivity profile is a result of threading the relatively long and flexible butylene moiety of Lys through the MT cavity facilitating hydrophobic interactions with the MTs' sidewalls, and simultaneous Coulombic attraction between the negatively charged bridgehead groups of the MTs and the ε-ammonium group of Lys.[16] Thus, we expected that by binding to Lys, MTs might compete with the combination of hydrophobic and electrostatic interactions that is important for oligomerization and aggregation of amyloidogenic proteins and prevent their toxicity. By selecting Lys as a target, we attempted to focus on the process of abnormal protein assembly itself rather than on a particular protein. Obviously, this raises the question of specificity and potential toxicity, because theoretically MTs would bind to any exposed Lys. However, we hypothesized that because their binding affinity is moderate, MTs might have sufficient power to disrupt the relatively weak interactions that nucleate aberrant self-assembly and at the same time not interfere with normal protein function, where binding energies typically are substantially higher. This "process-specific," rather than protein-specific, approach has not been explored to date.

EXPERIMENTAL SECTION

Materials. CLR01 and CLR03 were prepared and purified as described previously,[17] except that NaOH, rather than LiOH, was used in the final neutralization step to yield the sodium salt of each compound. Aβ40 and Aβ42 were purchased from the UCLA Biopolymers Laboratory. Islet amyloid polypeptide (IAPP) was obtained from PolyPeptide Laboratories, Torrance, CA. Calcitonin (CT) and PrP(106−126) were purchased from American Peptide, Sunnyvale, CA. β_2-microglobulin (β_2m) was obtained from Lee Biosolutions, St. Louis, MO. Insulin, transthyretin (TTR), and lysozyme were purchased from Sigma, St. Louis, MO.

A 0N3R (embryonic) tau-containing plasmid was transformed into competent BL21(DE3)+Rosetta *Escherichia coli* bacteria. Bacteria were inoculated in 2 L NZA medium containing ampicillin and chloramphenicol and incubated at 37 °C until the solution reached $OD_{600} = 0.5$. Tau expression was induced by addition of isopropyl-β-D-thiogalactoside and was allowed to continue for 3 h. The cells then were centrifuged at 10 000*g* for 10 min at 4 °C. The supernate was discarded and the pellet resuspended in 20 mL of lysis buffer (33 mM Tris-HCl, pH 8.0, 100 mM KCl + protease inhibitors). Cells were disrupted by 3× French pressing at 15 000 psi and centrifuged at 13 000*g* for 40 min at 4 °C. The supernate was boiled and then centrifuged again at 35 000*g* for 40 min at 4 °C. To precipitate proteins other than tau, 30% (w/v) ammonium sulfate was added to the supernate and the solution was agitated for 30 min at 4 °C. The supernate was collected after centrifugation at 20 000*g* for 30 min at 4 °C. Tau was precipitated by adding 40% ammonium sulfate and repeating the same process. The pellet was dissolved in BRB80 buffer (80 mM PIPES/KOH, 1 mM EGTA, 1 mM $MgCl_2$, pH 6.8) and protein purity was determined by SDS−PAGE and Coomassie blue staining.

Aggregation Assay. Each protein/peptide was dissolved in an appropriate buffer and incubated under suitable conditions for aggregation kinetics assays (Table 1) in the presence or absence of MTs. At different time intervals, aliquots of the aggregating solutions were taken out for ThT or turbidity measurements. A pretreatment with 1,1,1,3,3,3-hexafluoro-2-propanol (HFIP) (Sigma) was required for Aβ40, Aβ42, IAPP, and PrP(106−126) and was performed as described previously.[18] Dry peptide films were kept at −20 °C until use.

Thioflavin T (ThT) Fluorescence. ThT fluorescence was used to monitor the kinetics of β-sheet formation by Aβ, tau, IAPP, CT, insulin, and β_2m in the absence or presence of CLR01 or CLR03. Fifty microliter aliquots of the aggregation reaction were mixed with 300 μL of 20 μM ThT (Sigma) in 10 mM phosphate buffer (PB), pH 7.4, at different time points. The fluorescence was measured following 5 min incubation at λ_{ex} = 452 nm and λ_{em} = 485 nm, using a Hitachi F4500 spectrofluorometer (Hitachi Instruments, Rye, NH).[19] The data are presented as mean ± SEM of 3 independent experiments.

Turbidity. Time-dependent particle size growth of TTR and PrP-(106−126) was measured based on development of turbidity in the solution by monitoring the absorbance at 360 nm[20,21] using a DU640 spectrophotometer (Beckman, Brea, CA).

Electron Microscopy (EM). Experiments were done as described previously.[19] Briefly, 10-μL aliquots from the aggregation reactions in the absence or presence of CLR01 or CLR03 were spotted on glow-discharged, carbon-coated Formvar grids (Electron Microscopy Science, Hatfield, PA), fixed with 5 μL of 2.5% glutaraldehyde, and stained with uranyl acetate. The samples were analyzed using a CX 100 transmission electron microscope (JEOL, Peabody, MA).

Cell Culture. Rat pheochromocytoma (PC-12) cells were maintained in F-12 nutrient mixture with Kaighn's modification (F-12K) (Gibco BRL, Carlsbad, CA) supplemented with 15% heat-inactivated horse serum and 2.5% fetal bovine serum (FBS). Rat insulinoma (RIN5fm) cells were maintained in RPMI 1640 medium (Gibco BRL, Carlsbad, CA) supplemented with L-glutamine and 10% FBS. Cells were kept at 37 °C in an atmosphere of 5% CO_2.

Oligomeric Preparations of Proteins for Toxicity Assay. Following dissolution in an appropriate buffer, oligomers of the respective proteins were prepared using the conditions listed in Table 2. The oligomeric peptide/protein preparations then were added to cells at the listed concentration in the absence or presence of MTs, which were added just prior to adding to the cells, and incubated for 24 h. Cell viability was measured using the 3-(4,5-dimethylthiazol-2-yl)-2,5-diphenyltetrazolium bromide (MTT) reduction assay as described previously.[10] PC-12 cells were used for determining the toxicity of Aβ, CT, β_2m, TTR, and PrP(106−126), whereas RIN5fm cells were used for IAPP and insulin. For cell viability assays, PC-12 cells were incubated in 96-well plates at a density of 25 000 cells per well in differentiation media (F-12K, 0.5% FBS, 100 μM nerve growth factor) for 48 h. RIN5fm cells were trypsinized and plated in 96-well plates at a density of 20 000 cells per well in RPMI 1640 medium with 1% FBS. Cell viability was assessed quantitatively by the CellTiter 96 Non Radioactive Cell Proliferation Assay (Promega, Madison, WI). A positive control was 1 μM staurosporine for 100% reduction in cell viability, based on which the percentage viability of all of the experimental conditions was calculated. Plates were read using a Synergy HT microplate reader (BioTek, Winooski, VT) and the absorbance at 570 nm (formazan product) minus the absorbance at 630 nm (background) was recorded. Corrected absorbance

Table 1. Conditions Used for Aggregation Assays

protein (concentration in μM)	preparation	incubation conditions: temperature (°C)	incubation conditions: agitation	assay
Aβ40 (10)	Preparation A: HFIP-treated peptide films[18] were dissolved in 60 mM sodium hydroxide (10% of the final volume), followed by addition of 45% deionized water. The solution was sonicated for 1 min followed by addition of 20 mM PB (45% of the final volume)	25	+	ThT
Aβ42 (10)	Preparation A	25	+	ThT
Tau (4)	Tau stock solution (15.24 μM) was incubated with 5 mM dithiothreitol (DTT) for 10 min at room temperature followed by mixing with buffer containing 10 mM HEPES and 100 mM NaCl, pH 7.6, and incubated for an additional 15 min, after which 150 μM arachidonic acid (Sigma-Aldrich) was added to the reaction to initiate the fibrillization process.[30]	37	+	ThT
IAPP (10)	Preparation A	25	+	ThT
CT (25)	10 mM sodium phosphate, pH 7.4	37	+	ThT
Insulin (10)	10 mM glycine-HCl, pH 3.5	37	+	ThT
β_2m (20)	10 mM sodium acetate, pH 3.2	37	+	ThT
TTR (7.2)	10 mM sodium acetate, pH 4.4	37	-	Turbidity
PrP(106−126) (10)	Preparation A	25	+	Turbidity

Table 2. Oligomeric Preparations of different proteins for toxicity assay

protein (concentration added to cells in μM)	pretreatment before addition to cells: preparation conditions	oligomer preparation concentration (μM)	incubation: time (h)	incubation: temperature (°C)	incubation: agitation
Aβ40 (15)	Dissolved in minimal volume of 60 mM NaOH, followed by dilution in	100		none	
Aβ42 (10)	F-12K medium, pH 7.4.[49]	150		none	
IAPP (0.01)	Dissolved in minimal volume of 60 mM NaOH, followed by dilution in RPMI medium, pH 7.4.	1.12		none	
CT (15)	Dissolved in deionized water	1500	24	37	+
Insulin (5)	Dissolved in 10 mM glycine-HCl, pH 3.0. Modification of previously published protocol.[52]	1000	24	37	+
β_2m (10)	Dissolved in 10 mM sodium acetate, pH 3.2.	1500	24	37	+
TTR (1)	Dissolved in deionized water and dialyzed against sterile (autoclaved) water (pH 7−8) for 2 h. The resulting solution was diluted to 18 μM in sterile water.[53]	18	168	25	+
PrP(106−126) (10)	Dissolved in deionized water.	100		none	

was used to calculate the percent cell viability from the experimental change ($A_{media} - A_{experimental}$) over the dynamic range ($A_{media} - A_{staurosporine}$). The data are an average of 3 independent experiments with 5 wells per condition (n = 15).

Dot Blot Assay. Oligomers of Aβ42 were prepared in the absence or presence of MTs and probed by the oligomer-specific polyclonal antibody (pAb) A11 using a modification of previously described methods.[22] Briefly, HFIP-treated Aβ42 was dissolved in 60 mM NaOH at 2 mM. This solution was sonicated for 1 min followed by dilution with 10 mM PB to a final peptide concentration of 45 μM. The resulting solution was maintained at room temperature without agitation for 8 days. Periodically, 2-μL aliquots were applied to nitrocellulose membranes (Invitrogen, Carlsbad, CA). The membranes were blocked for 1 h with 5% nonfat milk in 10 mM Tris-buffered saline (TBS) followed by incubation with A11 at 1:1 000 dilution or monoclonal antibody (mAb) 6E10 (Covance, Princeton, NJ) at 1:10 000 dilution in TBS containing 5% nonfat milk followed by appropriate horseradish peroxidase-linked secondary polyclonal antibodies (Amersham Biosciences, Piscataway, NJ) and developed using an Enhanced Chemiluminescence (ECL) reagent kit (Amersham Biosciences).

Dynamic Light Scattering (DLS). DLS experiments were done as described previously[19] using an in-house built system with a He−Ne laser operating at 633 nm (Coherent, Santa Clara, CA) as a light source. The experiments were performed with 10 μM Aβ at Aβ/MT concentration ratios 1:10 or 1:1. Control experiments were performed with Aβ alone. Light scattered at 90° was collected using image transfer optics and detected by an avalanche photodiode built into a 256-channel correlator (Precision Detectors, Bellingham, MA). The size distribution of scattering particles was reconstructed from the scattered light correlation function using PrecisionDeconvolve deconvolution software (Precision Detectors) based on a regularization method by Tikhonov and Arsenin.[23]

Molecular Dynamics (MD). MD simulations were performed on a desktop PC using MacroModel 9.0 (Schrödinger, New York, NY).

Table 3. Amyloidogenic Proteins Used in the Present Study

protein	length (aa)	Lys	% Lys	Arg	% Arg	associated disease	reference
Aβ40, Aβ42	40, 42	2	5.0, 4.8	1	2.5, 2.4	AD	54
Tau (embryonic)	352	37	10.5	14	4.0	AD, tauopathies	54
α-Synuclein	140	15	10.7	0	0.0	PD, synucleinopathies	55
IAPP	37	1	2.7	1	2.7	Type-2 diabetes	56
CT	32	1	3.1	0	0.0	Medullary Carcinoma of the Thyroid	57
Insulin	51	2	3.9	1	2.0	Injection-related nodular amyloidosis	58
β_2m	99	8	8.1	5	5.1	Dialysis-related amyloidosis	59
TTR	147	8	5.4	5	3.4	Senile systemic amyloidosis, Familial amyloid polyneuropathy	60, 61
Lysozyme	130	5	3.8	13	10.0	Familial visceral amyloidosis	62
PrP(106−126)	21	2	9.5	0	0.0		63

The calculations assumed a temperature of 300 K and used the OPLS-2005 force field with water as the solvent (continuum solvation, GBSA).

Mass Spectrometry. Fifty micromolar solutions of Aβ40 or Aβ42 mixed with CLR01 at different concentration ratios in 100 mM ammonium bicarbonate, pH 7.6, were introduced into a Synapt HDMS quadrupole time-of-flight mass spectrometer (Waters, Milford, MA) by electrospray ionization (ESI) and analyzed as described previously.[24] Complexes were subjected to MS/MS fragmentation using ESI coupled with electron-capture dissociation (ECD) and Fourier transform-ion cyclotron resonance (ICR) MS (LTQ-FT Ultra, Thermo Scientific, San Jose, CA). The ions of interest were isolated in the linear ion trap and transferred into the ICR cell, where they were dissociated by activated ion ECD.[25]

NMR Spectroscopy and Titration. Lyophilized, uniformly ^{15}N- or [^{15}N, ^{13}C]-labeled Aβ40 (rPeptide, Bogart, GA) was suspended in 10 mM NaOH at a concentration of 2 mg/mL and sonicated for 1 min for disaggregation. This solution (60 μL) was diluted to 60 μM in 345 μL of 20 mM PB, pH 7.2, and 45 μL of D_2O. CLR01 and CLR03 were dissolved in PB at 25 mM and diluted into the Aβ sample. NMR experiments were carried out at 4 °C using Bruker 600 or 800 MHz spectrometers, each equipped with a triple-resonance cryogenic probe. NMR data were processed using NMRPipe[26] and analyzed using SPARKY (T. D. Goddard and D. G. Kneller, SPARKY 3, University of California, San Francisco, http://www.cgl.ucsf.edu/home/sparky/). ^{1}H−^{15}N Heteronuclear Single Quantum Coherence (HSQC) spectra were acquired on a 600 MHz spectrometer with 2048 (t_2) × 180 (t_1) complex data points, spectral widths of 7211 Hz in ^{1}H and 1581 Hz in ^{15}N, and 8 scans for each free induction decay. 2D ^{1}H−^{13}C(O) spectra of the HNC(O) experiments were acquired on an 800 MHz spectrometer with 2048 (t_2) × 128 (t_1) complex data points, spectral widths of 12 315 Hz in ^{1}H and 3333 Hz in ^{13}C, and 16 scans for each free induction decay. The recycle delay was 1.5 s. The resonance assignments of free Aβ40 have been reported previously.[27]

RESULTS

We selected nine different human, disease-associated amyloidogenic peptides/proteins (Table 3), including Aβ (both Aβ40 and Aβ42), tau (embryonic isoform), α-synuclein, IAPP, CT, insulin, β_2m, TTR, and lysozyme. We also studied the amyloidogenic peptide PrP(106−126). Results for α-synuclein are reported elsewhere[28] and it is included here for comparison. Of these proteins, Aβ, tau, α-synuclein, IAPP, calcitonin, and PrP(106−126) have been reported to be unstructured in aqueous solutions in the absence of structure-stabilizing additives, whereas insulin, β_2m, TTR, and lysozyme have a stable structure under normal physiological conditions.

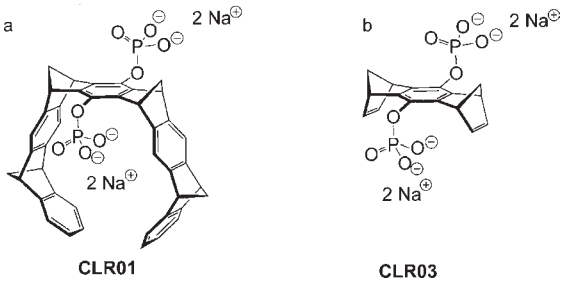

Figure 1. Molecular structures of MTs: (a) CLR01; (b) CLR03. These compounds are slightly basic in aqueous solution and the phosphate groups are partially protonated at pH 7.4.

Initial examination of several MT derivatives has led to selection of a lead compound called CLR01[16] (Figure 1a). A truncated derivative, CLR03[17] (Figure 1b), which cannot "embrace" the Lys side chain, was predicted to be inactive and therefore used as a negative control. CLR01 forms unique host−guest complexes with lysine derivatives by including the $H_3N^+-CH_2-CH_2-CH_2-CH_2$ side chain inside its own cavity. Host−guest complexes of CLR01 with Arg derivatives are significantly less stable (Supplementary Table S1).

CLR01 Inhibits Amyloid Formation. Our first set of experiments used the proteins involved in AD, Aβ, and tau. To test the effect of MTs on the aggregation of these proteins, we incubated Aβ40, Aβ42, or tau in the absence or presence of CLR01 or CLR03 and monitored β-sheet formation by ThT fluorescence[29] and morphological changes by EM. The Aβ analogues aggregated spontaneously, whereas tau was induced to aggregate by arachidonic acid.[30] In the absence of MTs, following a lag phase of ∼10 or ∼3 h for Aβ40 and Aβ42, respectively, the ThT fluorescence increased gradually until it reached a plateau by ∼75 or ∼30 h (Figure 2a,b). For tau, the increase in ThT fluorescence signal began immediately following induction and reached a plateau by ∼15 h (Figure 2c). At 1:10 Aβ/CLR01 or 1:1 tau/CLR01 concentration ratios, little or no change in ThT fluorescence intensity was observed, suggesting inhibition of β-sheet formation. Examination of the protein morphology by EM showed that Aβ and tau samples incubated in the absence of MTs formed abundant fibrils, whereas in the presence of CLR01, no fibrils formed (Figure 2d−f). As expected, CLR03 did not inhibit Aβ or tau fibrillogenesis or β-sheet formation, supporting the necessity of the hydrophobic sidewalls for specific binding to Lys and inhibiting aggregation. We also validated the data for Aβ using

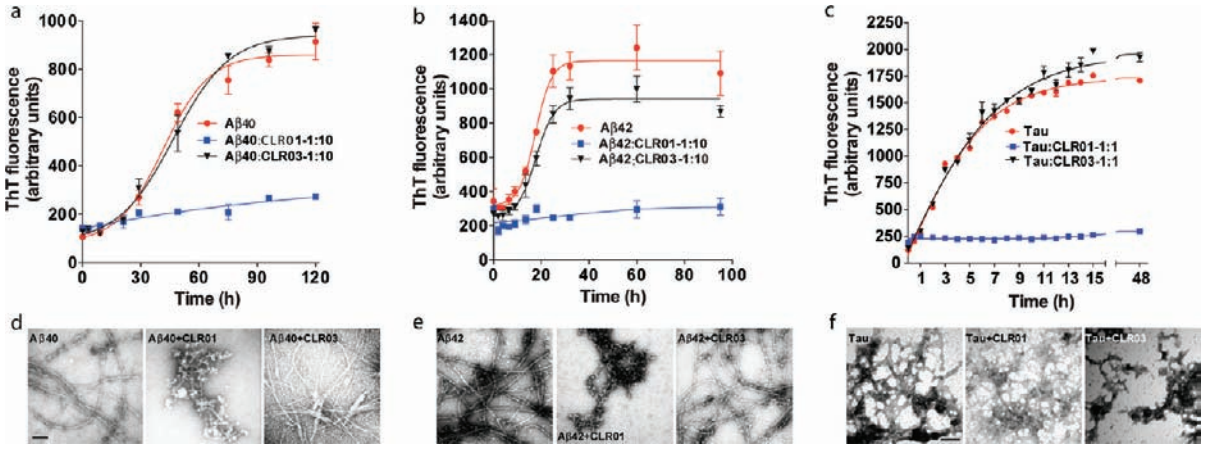

Figure 2. CLR01 inhibits Aβ and tau aggregation. The effect of MTs on β-sheet formation by (a) Aβ40, (b) Aβ42, and (c) embryonic tau was assessed by measuring ThT fluorescence. The data are presented as mean ± SEM of three independent experiments. Morphological analysis of (d) Aβ40, (e) Aβ42, and (f) tau in the absence or presence of MTs was examined at the end of each aggregation reaction. Scale bars indicate 100 nm.

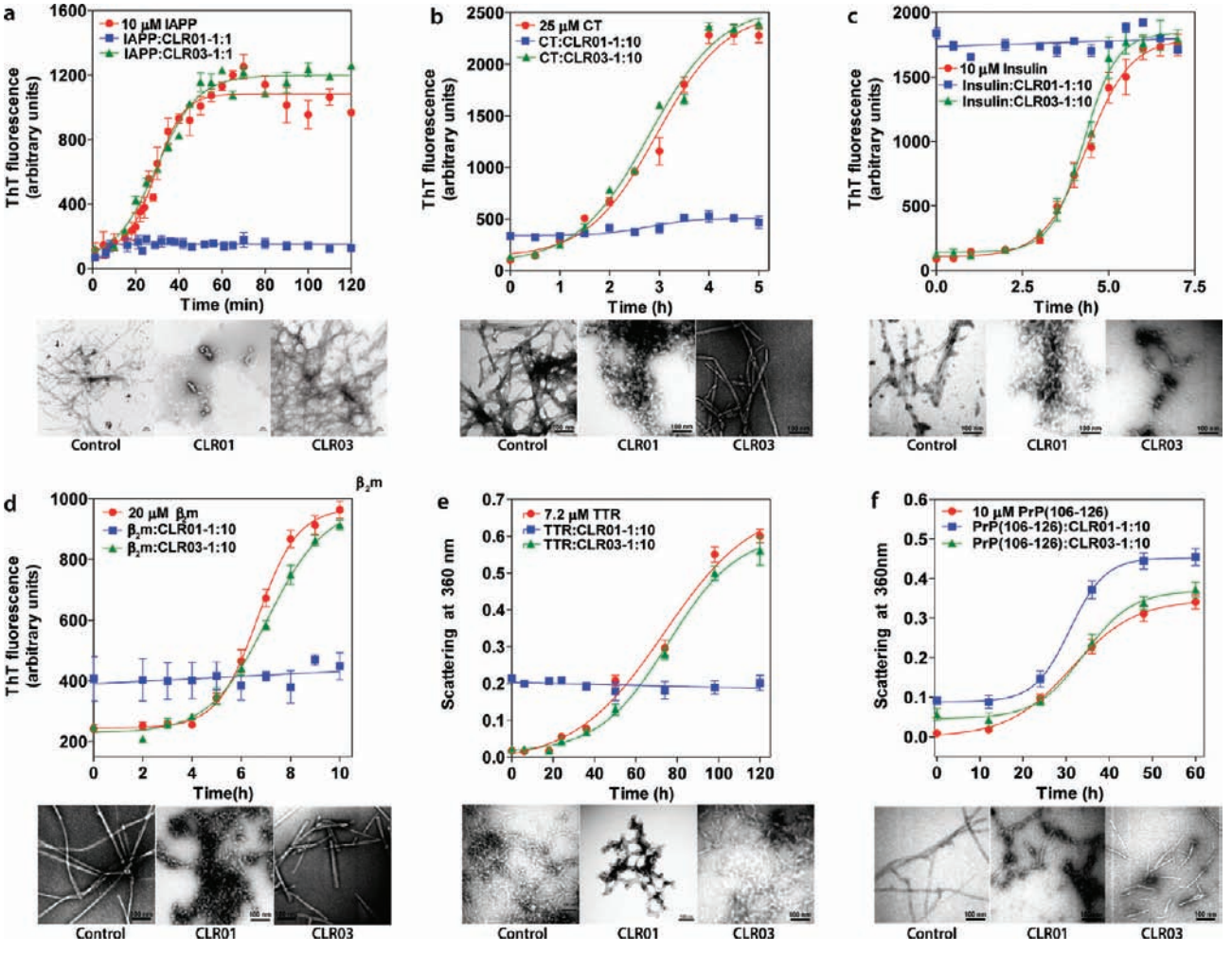

Figure 3. CLR01 inhibits assembly of multiple amyloidogenic proteins. IAPP, CT, insulin, β_2m, TTR, or PrP(106−126) was incubated in the absence or presence of the indicated amount of CLR01 or CLR03. The reactions were monitored by ThT fluorescence or turbidity as indicated in each panel. The data represent mean ± SEM of three independent experiments. At the completion of each aggregation reaction, aliquots were spotted on carbon-coated grids and examined by EM.

CD spectroscopy (Supplementary Figure S1). Dose-dependence analysis showed complete inhibition of β-sheet formation in 10 μM Aβ42 or Aβ40 by 3-fold excess CLR01 and partial inhibition at a 1:1 concentration ratio (Supplementary Figure S2). The lower

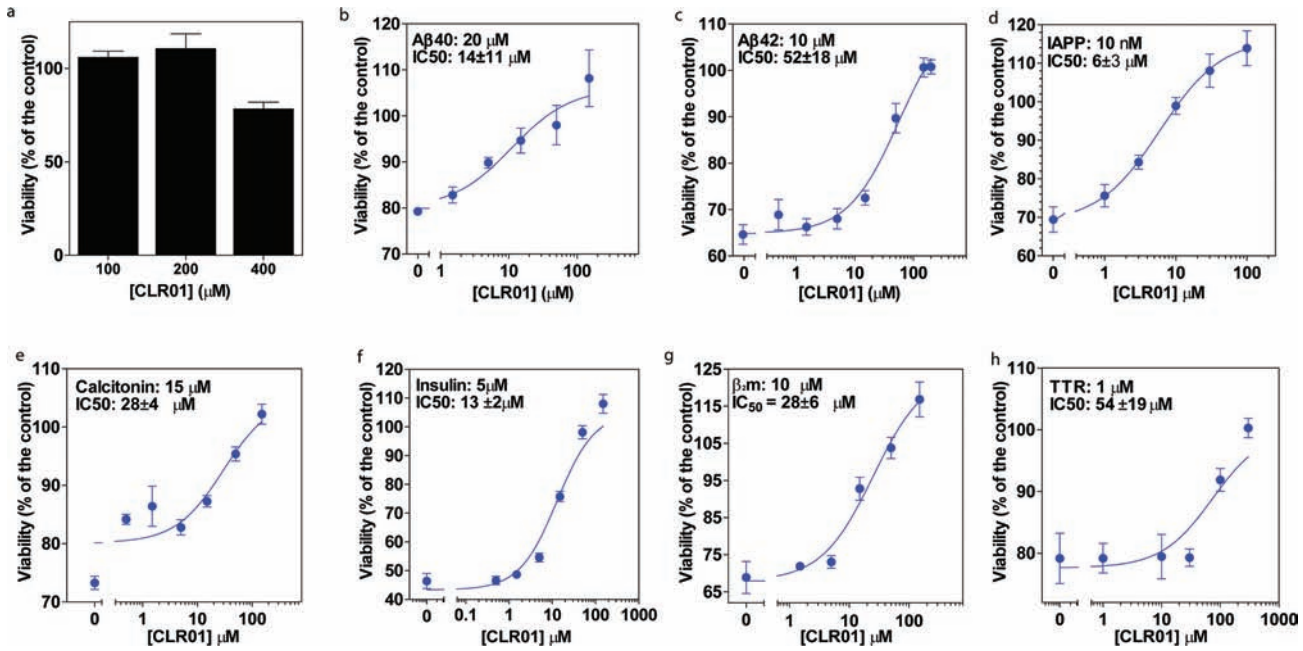

Figure 4. Dose-dependent inhibition of toxicity of amyloidogenic proteins by CLR01. (a) Increasing concentrations of CLR01 were incubated with differentiated PC-12 cells for 24 h and cell viability was measured using the MTT reduction assay. The data are presented as mean ± SEM of three independent experiments. (b−h) Oligomeric preparations of each protein, at the concentration indicated in the appropriate panel, were added to differentiated PC-12 or RIN5fm cells in the absence or presence of increasing CLR01 concentrations. Cell viability was measured using the MTT assay. The data are presented as mean ± SEM of three independent experiments.

protein/CLR01 molar ratio needed for complete inhibition of tau aggregation (1:1) than of Aβ (1:3) correlates with the higher relative abundance of Lys in the tau sequence (10.5%) relative to Aβ (5.0%/4.8% in Aβ40/Aβ42, respectively, Table 3).

In view of the results described above, we asked to what extent the inhibition of aggregation by CLR01 was a general phenomenon. To answer this question, we used structured and unstructured proteins of various sizes known to form amyloid in human diseases. On the basis of the number, location, and relative abundance of Lys residues in each protein (Table 3 and Supplementary Figure S3), we expected that CLR01 would inhibit the aggregation of α-synuclein, insulin, β_2m, TTR, and lysozyme, but not of IAPP, which contains a single Lys residue at position 1. CT also has only one Lys residue, but this residue, Lys18, is within a sequence previously reported to be important for amyloid formation,[31−33] and therefore, we predicted that CLR01 might be able to inhibit CT aggregation. It was difficult to predict the impact of CLR01 on PrP(106−126), which has two Lys residues corresponding to 9.5% of its sequence, but are located in positions 1 and 5, away from the hydrophobic, amyloidogenic region at the C-terminus.

To measure inhibition of amyloid fibril formation by CLR01, we used morphological examination by EM and ThT fluorescence as described above. However, for TTR and PrP(106−126) an increase in ThT fluorescence upon fibril formation was not detected. Therefore, we used turbidity at λ = 360 nm to measure the aggregation kinetics in these cases instead. As an initial screen, we tested the effect of 10-fold excess CLR01 or CLR03 on each protein (except IAPP). In agreement with our predictions, CLR01, but not CLR03, inhibited the fibrillogenesis of CT, insulin, β_2m, and TTR (Figure 3). As reported elsewhere,[28] CLR01 also inhibited efficiently the aggregation of α-synuclein. Surprisingly, contrary to our prediction, CLR01 was found to inhibit the aggregation of IAPP at a 1:1 concentration ratio. Therefore, higher concentration ratios were not tested.

The conditions under which lysozyme forms fibrils *in vitro*, namely, 1.5 mM concentration and pH 2,[34] were found to be unsuitable for inhibition by CLR01. The pK_a of phosphate groups is ~2.15. Therefore, at pH 2, the phosphate groups of CLR01 are protonated, and consequently, the aqueous solubility of the compound is below usable concentrations. Thus, studies with lysozyme could not be executed.

Interestingly, in some cases, the baseline ThT fluorescence or turbidity in the presence of CLR01 at t = 0 was higher than in the absence of CLR01. A possible explanation for this increase in initial ThT fluorescence or turbidity is that CLR01 induced rapid formation of soluble assemblies with amorphous morphology and increased β-sheet content, similar to the "fibrillar oligomers" described by Glabe et al.[35] or the Aβ oligomers reported by Chimon et al.[36] This phenomenon was particularly notable in experiments using insulin, in which the fluorescence in the presence of CLR01 at t = 0 was as high as that of insulin incubated in the absence of CLR01 at the end of the aggregation reaction (Figure 3c). However, EM examination showed that fibrils did not form in the presence of CLR01. A close look at the morphology of insulin at t = 0 revealed the presence of microcrystals (Supplementary Figure S4). In the presence of CLR01, the microcrystals appeared eroded immediately following addition of the compound, as if CLR01 rapidly disaggregated the insulin microcrystals. Presumably, the resulting highly concentrated amorphous assemblies around the microcrystals bound ThT and gave rise to the high fluorescence observed at t = 0. Alternatively, a ternary complex of insulin, CLR01, and ThT might have formed giving rise to the high initial ThT fluorescence.

In the case of PrP(106−126), CLR01 and CLR03 had a similar, relatively mild effect on the time-dependent increase in turbidity,

Table 4. CLR01 Inhibits Toxicity of Amyloidogenic Proteins

protein	concentration in toxicity assay (μM)	cells	IC_{50} (μM)	IC_{50}/conc.
Aβ40	20	PC-12	14 ± 11	0.7
Aβ42	10	PC-12	52 ± 18	5.2
α-Synuclein	20	PC-12	3 ± 1	0.15
IAPP	0.01	RIN5fm	6 ± 3	600
CT	15	PC-12	28 ± 4	1.9
Insulin	5	RIN5fm	13 ± 2	2.8
β_2m	10	PC-12	28 ± 6	2.8
TTR	1	PC-12	54 ± 19	54

suggesting little or no inhibition of aggregation (Figure 3f). However, the morphology of PrP(106−126) in the presence of CLR01 was a mixture of short, worm-like fibrils and amorphous aggregates, whereas in the absence of MTs or in the presence of CLR03, abundant fibrils formed. Thus, despite a small effect of CLR01 on PrP(106−126) aggregation kinetics, the compound partially prevented formation of amyloid fibrils.

In all the cases in which CLR01 was found to inhibit aggregation at 10-fold excess in our initial screen, we characterized further the ratio of protein/CLR01 needed for inhibition of aggregation using ThT fluorescence or turbidity measurements. We found in most cases complete inhibition at 1:1 and partial inhibition at 10:1 protein/CLR01 concentration ratio (Supplementary Figure S5). These observations suggested that CLR01 inhibited both the nucleation and the elongation of fibril formation by these proteins.

CLR01 Inhibits Toxicity of Amyloidogenic Proteins in Cell Culture. We tested next whether CLR01 protected cultured cells against toxicity induced by the amyloidogenic proteins under consideration. Differentiated PC-12 cells were used to study the toxicity induced by Aβ, CT, β_2m, TTR, and PrP(106−126), whereas RIN5fm cells were used to characterize IAPP and insulin toxicity. We used the MTT reduction assay for measurement of cell viability in all cases. Before initiating inhibition experiments, we tested whether CLR01 itself was toxic to the cells. As explained above, MTs potentially can bind to any exposed Lys and at sufficiently high concentration could disrupt many cellular processes. Therefore, it was important to determine whether a sufficient window existed between CLR01 concentrations that reduced cell viability and those needed for inhibition of toxicity caused by amyloidogenic proteins. We found that, in PC-12 cells, CLR01 increased cell viability by 5−15% relative to control cells at concentrations up to 200 μM (Figure 4a) and caused ∼25% decrease in cell viability at 400 μM. Therefore, in subsequent inhibition experiments, we kept CLR01 concentration below 400 μM.

To measure inhibition of toxicity, proteins were incubated under conditions promoting oligomer formation (Table 2) and mixed with CLR01 or CLR03 immediately prior to adding to the cells. Cell viability was measured following 24 h of incubation. This type of assay is physiologically relevant for Aβ, CT, insulin, β_2m, and TTR, and is a reasonable choice for PrP(106−126). Exogenous addition would be physiologically irrelevant for tau, and hence, the experiment was not conducted with tau. In our initial screen, we found that the toxic insult caused by each protein was inhibited by CLR01 at concentrations below 400 μM, except for PrP(106−126) where CLR01 showed only mild protection. Increasing the PrP(106−126)/CLR01 concentration ratio up to 1:30 did not result in higher cell viability. CLR03 had no effect in all cases, as expected (Supplementary Figure S6).

Subsequent dose-dependent inhibition experiments were used to calculate the CLR01 concentration required for half-maximal inhibition (IC_{50}) in each case (Figure 4 and Table 4). As the proteins/peptides were added exogenously at different concentrations to the cells, the IC_{50} values of CLR01 depended on the concentration of the respective protein and should be considered relative to that concentration. In most cases, the IC_{50} value was in the same order of magnitude as the protein concentration used. Two exceptions were TTR and IAPP, for which the concentration of CLR01 needed for inhibition was 1- or 2-orders of magnitude higher than the protein concentration, respectively. Considering that the *in vivo* concentration of most of the amyloidogenic proteins studied here is in the nanomolar range, the data suggest that CLR01 may inhibit the toxic effect of these proteins *in vivo* at concentrations several orders of magnitude below its toxic concentration.

CLR01 modulates Aβ oligomerization. In subsequent experiments, we aimed to explore the mechanism by which CLR01 interacts with amyloidogenic proteins and the impact of its binding on the self-assembly process. We focused these experiments on Aβ as an archetypal amyloid protein. Some experiments were done with both Aβ40 and Aβ42, whereas others used only Aβ42 as the more amyloidogenic and toxic Aβ form.

Because the most toxic species of Aβ (and likely other amyloidogenic proteins) are believed to be soluble oligomers,[37] we asked next how CLR01 affected Aβ oligomerization. Aβ42 oligomers were prepared according to Necula et al.[22] and incubated in the absence or presence of MTs. Oligomer formation was examined by dot blotting using the oligomer-specific pAb A11.[38] An identical membrane was probed with the Aβ-specific mAb 6E10 as a loading control (Figure 5a). In the absence of MTs, A11 immunoreactivity was observed already at $t = 0$ h and increased up to 120 h. In contrast, Aβ42 samples incubated in the presence of CLR01 did not show A11 reactivity. As expected, CLR03 had no effect. The lack of A11 reactivity in the presence of CLR01 already at $t = 0$ suggested that the reaction of CLR01 with Aβ was fast and induced structural changes precluding formation of the toxic oligomers recognized by A11. It is possible also that binding of CLR01 masked A11 epitopes preventing recognition of Aβ oligomers by the antibody. However, this is unlikely because A11 is a polyclonal antibody.

The combination of the data described above suggested that CLR01 interacted with Aβ rapidly and modulated the aggregation process toward formation of nontoxic oligomers. To investigate the impact of CLR01 on the oligomer size distribution of Aβ directly and noninvasively, we used dynamic light scattering (DLS). Previously, immediately following preparation, Aβ40 and Aβ42 had been shown to form particle distributions with hydrodynamic radii (R_H) = 2−6 and 8−10/20−60 nm, respectively, which grew in size over several days as each peptide aggregated.[19] In initial experiments using a 1:10 Aβ/CLR01 concentration ratio, respectively, similar particle distributions were observed initially, but no particle growth was detected for over a month (data not shown).

In follow-up experiments, we tested the effect of CLR01 or CLR03 on Aβ42 assembly at a 1:1 concentration ratio. A moderate increase in the abundance of Aβ42 particles of R_H = 8−10 and 20−60 nm was observed relative to Aβ42 prepared in the absence of MTs (Figure 5b). However, growth of larger aggregates (R_H =500−1000 nm), which was prominent in the absence of MTs, was substantially suppressed in the presence of CLR01. Interestingly, in the presence of CLR03, formation of aggregates of R_H =500−1000 nm was somewhat accelerated. The data

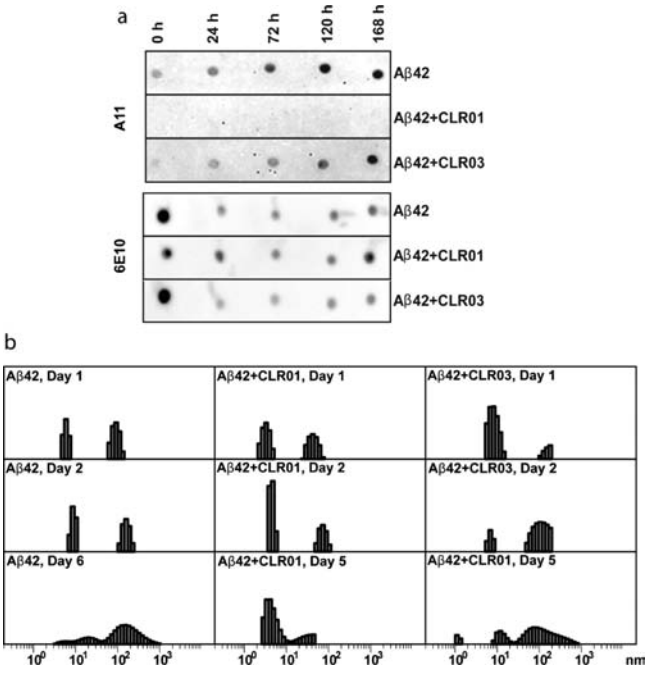

Figure 5. CLR01 modulates Aβ42 oligomerization. (a) Aβ42 oligomers were prepared as described in the Experimental Section in the absence or presence of CLR01 or CLR03 and incubated up to 8 days. Immunoreactivity was probed using pAb A11 or mAb 6E10 as a loading control. (b) Aβ assembly size distribution in the presence or absence of MTs was monitored using DLS. Ten micromolar Aβ42 was incubated with 10 μM CLR01 or CLR03 at room temperature with no agitation and particle size distribution was monitored for 5−6 days.

supported the interpretation that CLR01 stabilized nontoxic oligomeric Aβ populations, preventing their aggregation, and revealed that these particle populations were comparable in size to those formed by Aβ alone.

To glean additional insight into the effect of CLR01 binding on Aβ oligomerization, we performed molecular dynamics (MD) simulations using Aβ42 with starting conformation based on solid-state NMR (ssNMR) data by Lührs et al.[36] in the absence or presence of CLR01 (Supplementary Figure S7). In the beginning of the simulations, two Aβ monomers were positioned parallel to each other and separated by a distance of 8 Å. Following simulation for 1 ns, the two monomers associated with each other and established most of the intermolecular ion pairs and hydrogen bonds found in the ssNMR structure. In contrast, Lys28 complexation by CLR01 prevented any intermolecular interactions after 1 ns of simulation.

CLR01 Disintegrates Preformed Aβ Fibrils. Next, we tested if CLR01 could disaggregate preformed Aβ fibrils. Ten-fold excess CLR01 was added to solutions of Aβ40 or Aβ42 at two different time points during fibril maturation—an early time point, in which immature fibrils were still forming, and a late time point, in which abundant mature fibrils were present. In both cases, we found that CLR01 disaggregated the fibrils slowly yet efficiently (Figure 6) suggesting that CLR01 might dissolve amyloid plaques *in vivo*. Similarly, CLR01 was found to disaggregate preformed α-synuclein[28] and IAPP[39] fibrils.

CLR01 Binding Sites on Aβ Though multiple inhibitors of amyloidogenic proteins in general, and Aβ in particular, have been described in the literature, the mode of interaction and binding sites of such inhibitors are largely unknown. In contrast,

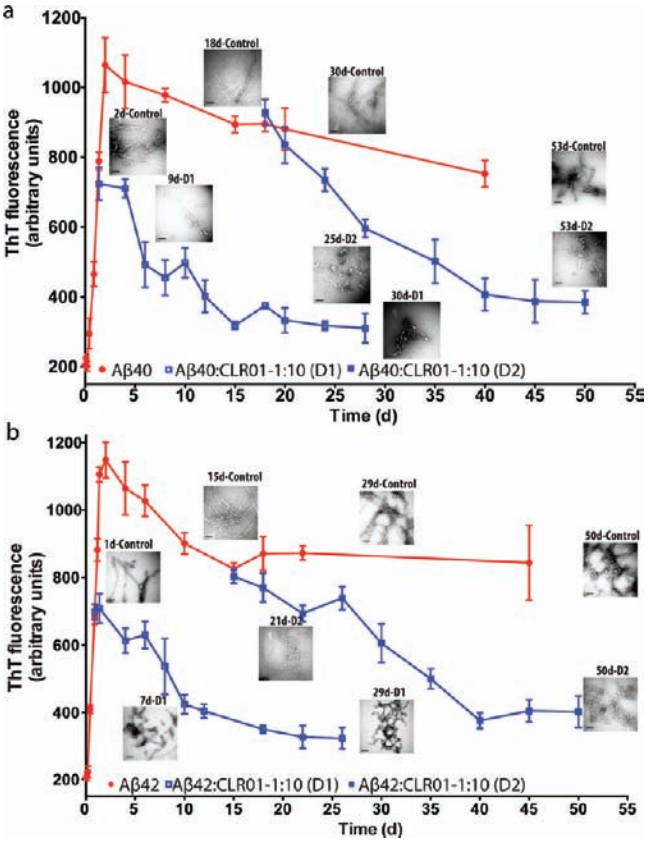

Figure 6. CLR01 disaggregates Aβ fibrils. Disaggregation of preformed (a) Aβ40 or (b) Aβ42 fibrils by CLR01 was studied by adding 10-fold excess CLR01 to aggregating solutions of 10 μM Aβ40 or Aβ42 at 21 h (disaggregation reaction D1) or 15 days (D2) after initiation of aggregation. The reactions were monitored using ThT fluorescence and EM. The micrographs show the morphology in samples incubated in the absence or presence of CLR01 at different time points. Scale bars indicate 100 nm.

MTs were chosen based on their known binding specificity for Lys. Aβ contains two Lys and one Arg residues, at positions 16, 28, and 5, respectively. CLR01 was expected to bind each of these residues and have higher affinity for Lys than for Arg (ref 16 and Supplementary Table S1). The actual affinity for each residue would result from a combination of intrinsic affinity and steric accessibility. To determine the binding sites of CLR01 on Aβ, we used two independent methods—mass spectrometry coupled with electron capture dissociation (ECD-MS), and solution-state NMR.

Electrospray ionization coupled with ECD and Fourier transform-ion cyclotron resonance (ICR)MS provides sequence data by scission of peptide bonds while keeping noncovalent complexes intact.[24] To explore the binding sites of CLR01 on Aβ, 50-μM solutions of Aβ40 or Aβ42 were mixed with CLR01 at different concentration ratios. In samples containing 100 μM CLR01, we observed Aβ complexes with up to 3 bound CLR01 molecules (data not shown), suggesting binding at all three possible locations, Lys16, Lys28, and Arg5. The 1:1 Aβ/CLR01 complexes could be enriched by lowering CLR01's concentration to 50 μM (i.e., 1:1 concentration ratio). The ions of interest were isolated in a linear ion trap and transferred to the ICR cell where they were subjected to ECD followed by MS/MS fragmentation. Figure 7 shows a schematic MS/MS fragmentation profile of the 4+-charged, 1:1 Aβ40/CLR01 and Aβ42/CLR01

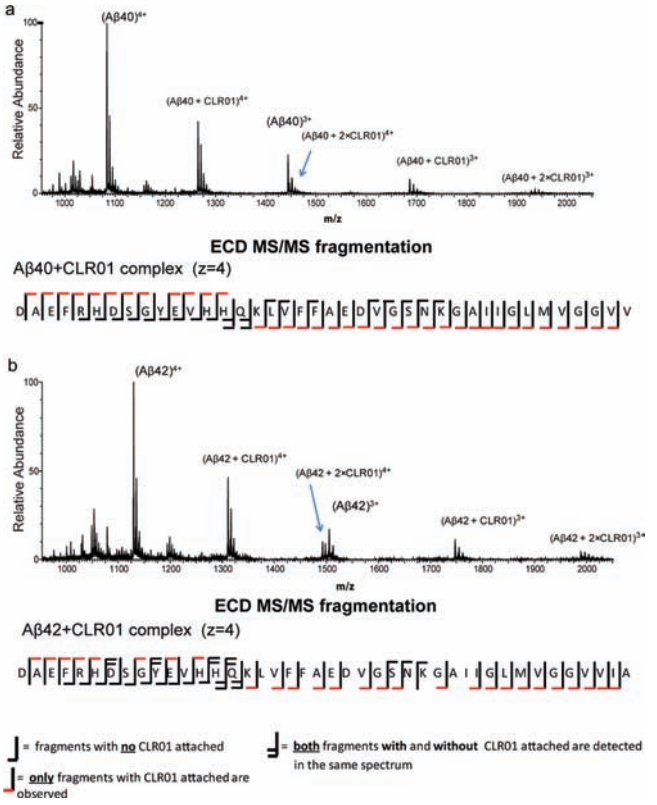

Figure 7. Binding sites of CLR01 on Aβ investigated by ECD-MS. Mass spectra are shown at the top of each panel. Schematic MS/MS fragmentation profile of (a) the 4+-charged 1:1 Aβ40/CLR01 complex and (b) Aβ42/CLR01 complex are shown below each spectrum. Aβ fragments of the *c*- (retaining the N-terminus) and *z**- (retaining the C-terminus) product ion series were observed in each case. Some product ions from dissociation of the polypeptide backbone corresponded to unbound peptide (single black line), whereas other product ions retained binding to CLR01 (single red line). At some positions along the peptide chain, product ions were observed in both CLR01-bound and unbound states (double black lines).

complexes below each spectrum. Aβ fragments of the *c*- (retaining the N-terminus) and *z**- (retaining the C-terminus) product-ion series were observed. Some product ions from dissociation of the polypeptide backbone corresponded to unbound peptide, whereas other product ions retained binding to CLR01. At some positions along the peptide chain (indicated by double black lines), product ions were observed in both CLR01-bound and unbound states. The observation of CLR01-bound *c*-product ions containing Lys16 (*c16*) and CLR01-bound *z**-product ions containing His14 (*z27*) in Aβ40 indicated that CLR01 bound within the Aβ(14−16) region, most likely at Lys16. Similar results were observed in Aβ42, where CLR01-bound *c*- and *z**-product ions were observed to contain Lys16 (*c16*) and His 13 (*z30*), respectively, suggesting that the binding was located in Aβ(13−16), most likely at Lys16.

In NMR experiments with full-length Aβ, we used Aβ40 because its higher aqueous solubility relative to Aβ42 facilitated obtaining high-quality spectra. Aβ40 concentration was kept constant at 60 μM and CLR01 concentration was increased from 6 to 30 μM. ^{1}H−^{15}N and ^{1}H−^{13}C Heteronuclear Single Quantum Coherence (HSQC, H(N)CO) 2D-NMR experiments were performed using Aβ40 at 60 μM in the absence (Figure 8a) or

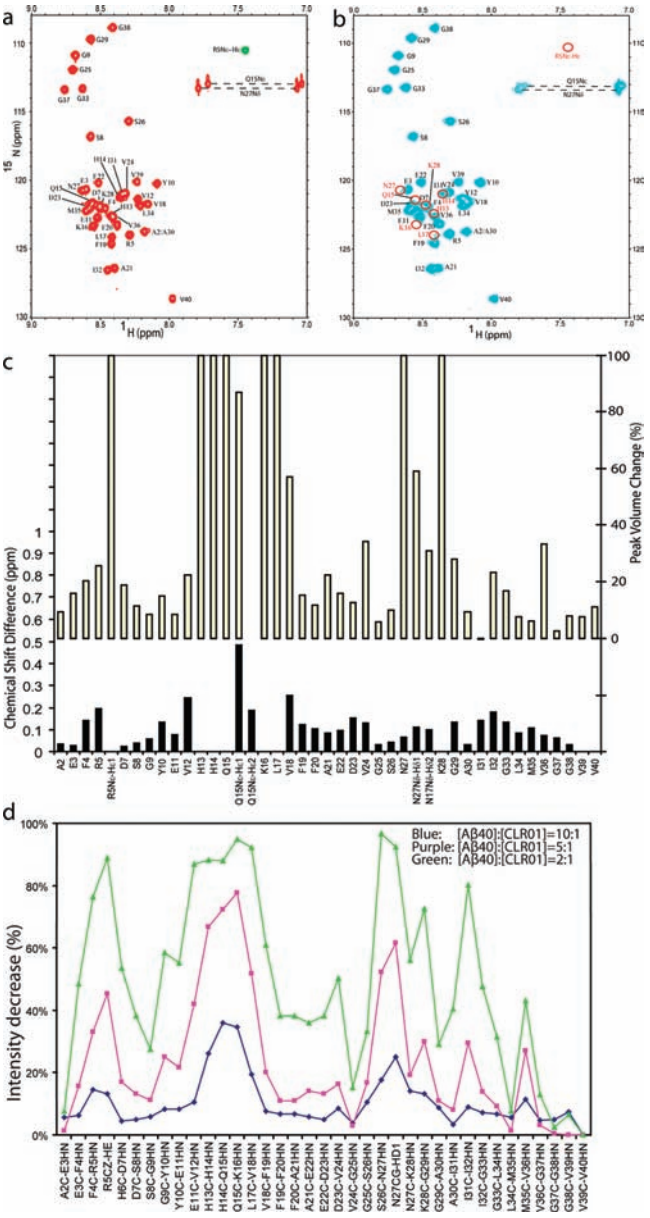

Figure 8. CLR01 binding sites on Aβ determined by solution-state 2D-NMR. (a) ^{15}N−^{1}H spectrum of Aβ40 alone (red or green). (b) ^{15}N−^{1}H spectrum of Aβ40 in the presence of 30 μM CLR01 (cyan). Red circles indicate resonances that disappeared completely upon addition of CLR01. (c) Resonance perturbation upon addition of 30 μM CLR01 to 60 μM Aβ40. (d) Aβ40/CLR01 mixtures were analyzed by 2D solution-state H(N)CO NMR experiments. Aβ40 concentration was kept constant at 60 μM and CLR01 concentration was increased from 6 to 30 μM.

presence (Figure 8b−d) of different concentrations of CLR01. These experiments showed substantial perturbation of resonances already at an Aβ40/CLR01 concentration ratio 10:1, respectively (Figure 8d). The degree of perturbation was largest in residues surrounding Lys16 and Lys28. In addition, we observed the disappearance of the side chain, but not the backbone, NH resonance of Arg5 (cf. Figure 8, panels a and b). The observed decrease in peak intensities were likely due to the line-broadening effect of CLR01 binding. The NMR data suggested that binding of CLR01 occurred predominantly at the two Lys residues and to a lesser extent at Arg5, as expected. Importantly, the data demonstrated

binding of CLR01 to Aβ monomers, already at a 10:1 Aβ/CLR01 concentration ratio, respectively. At higher concentrations of CLR01, resonances along the entire sequence were perturbed (Figure 8c,d), likely due to self-assembly of Aβ into oligomers, a conclusion supported by the observation of particle populations consistent with oligomers at the earliest time points in the DLS experiments (Figure 5b). In the presence of CLR03 at concentrations up to 240 μM, no resonance perturbation was observed (Supplementary Figure S8).

In other ^{1}H NMR experiments, we used CLR01 and Aβ(15−29) at 4:1 concentration ratio, respectively. In these experiments, the specific inclusion of Lys side chains as guests inside the host MT cavity was detected directly by a large, complexation-induced shift of the guest signals $\Delta\delta_{max}$ (Supplementary Figure S9) assigned to the δ- and ε-methylene groups of Lys. In contrast, the ^{1}H NMR chemical shifts of all other amino acid subunits were not affected. The $\Delta\delta_{max}$ values (∼−4 ppm) found for the complexed Lys subunits in Aβ(15−29) matched those observed for smaller Lys derivatives (Supplementary Table S1).

DISCUSSION

Diseases of aberrant protein folding and assembly are a tremendous threat to global public health. Over 35 million people suffer from AD alone, and the numbers of patients are increasing steeply threatening to create a global financial crisis.[40] Effective inhibition or modulation of the aberrant assembly process therefore is an appealing strategy for preventing and/or treating these diseases. Achieving this goal, however, is complicated due to the metastable nature of amyloidogenic protein oligomers and the unfavorable characteristics of amyloid fibrils as targets.[41,42] Though amyloidogenic proteins comprise distinct amino acid sequences, amyloid fibrils[2] and oligomers of amyloidogenic proteins[38] each share a great deal of structural similarity, which largely is sequence-independent. It is therefore not surprising that inhibitors have been found to arrest the aggregation of more than one protein.[43,44] However, to our knowledge, this is the first study in which compounds were sought using a rational approach with the goal to obtain agents that inhibit general amyloid protein assembly and toxicity in a process-specific manner.

On the basis of the idea of targeting an amino acid residue that participates in all types of the key interactions involved in the nucleation, oligomerization, and elongation processes, we used Lys-specific MTs and found a lead compound, CLR01, which is capable of disrupting the aggregation and toxicity of multiple disease-related proteins. CLR01 was found to inhibit formation of amyloid fibrils by proteins related to AD (Aβ and tau, Figure 2), PD (α-synuclein),[28] T2D (IAPP), and several other amyloid-related diseases (Figure 3). In most cases, the inhibition of aggregation correlated with inhibition of toxicity of these proteins in cell culture (Figures 3 and 4 and Table 4), suggesting that both were mediated by CLR01 binding to exposed Lys residues and preventing their intra- and intermolecular interactions. Importantly, our toxicity experiments were designed to assess inhibition of the harmful action of toxic oligomers rather than the disruption of the oligomers themselves. Thus, proteins were incubated under conditions that promote oligomerization and CLR01 was added to this preparation immediately before addition to the cells. The data suggest that CLR01 indeed inhibits the toxicity of the oligomers, either by rapidly modulating them into nontoxic structures or by preventing their interaction with their cellular targets.

An exception to the list of proteins inhibited by CLR01 was PrP(106−126), which contains two Lys residues at the N-terminus, away from the long amyloidogenic C-terminal sequence, providing little opportunity for CLR01 binding to interfere with the aggregation. Thus, despite modulating the aggregation of PrP(106−126) into predominantly nonfibrillar structures, CLR01 had little effect on PrP(106−126) aggregation kinetics as measured by turbidity (Figure 3) and only partially attenuated PrP(106−126)-induced toxicity at ≥10-fold excess (Figure 4). This result, however, does not exclude the possibility that CLR01 may inhibit the conversion of full-length human PrP, which contains 10 Lys residues corresponding to 4.8% of the sequence, from the soluble, cellular form, PrP^C, to the insoluble, toxic, and infectious scrapie form, PrP^{Sc}. We also could not study the inhibition of lysozyme aggregation by CLR01 because *in vitro* lysozyme aggregation requires very low pH and high concentration, which are incompatible with CLR01 solubility. However, *in vivo* lysozyme aggregates at physiologic pH and substantially lower concentrations and its aggregation may be inhibited by CLR01.

The observation that CLR01 inhibited IAPP aggregation and toxicity was surprising because IAPP has a single N-terminal Lys, away from the sequences known to be involved in the amyloid core.[45] Moreover, CLR01 appeared to inhibit IAPP aggregation effectively, even at substoichiometric concentrations. However, unlike with most of the other proteins examined, for which the concentration required for inhibition of aggregation was similar to that needed for inhibition of toxicity, in the case of IAPP, high excess CLR01 was needed for inhibition of toxicity. This discrepancy between the stoichiometries of inhibition of aggregation and toxicity suggests that interactions other than CLR01 binding to Lys1 in IAPP may mediate the inhibition. Subsequent studies support this hypothesis and will be reported elsewhere in the near future.[39]

How inhibitors of protein aggregation bind to their targets and what structures form as a result of inhibitor binding are difficult questions to answer. Here, we used Aβ as a model protein for elucidating the structural details of CLR01 binding and its effect on the resulting assemblies. We found that CLR01 stabilized oligomeric Aβ structures that were similar in size (Figure 5b) to those forming in the absence of CLR01. Nevertheless, unlike the Aβ oligomers formed in the absence of inhibitors, those that formed in the presence of CLR01 did not bind A11 (Figure 5a) and were not toxic to differentiated PC-12 cells. These observations suggest that CLR01 modulates the structure of early Aβ assemblies in a subtle way that cannot be detected easily by gross morphological or spectroscopic methods, such as EM or DLS, but is sufficient to render the resulting assemblies nontoxic and prevent their further aggregation. Notably, stabilization of nontoxic oligomers appears to be a general mechanism for inhibitors of Aβ assembly and toxicity, including *scyllo*-inositol,[46] epigallocatechin gallate,[43] resveratrol[47] and other polyphenols,[48] and peptides derived from the C-terminus of Aβ42.[49,50] If this mechanism is found to be applicable to other amyloidogenic proteins, the data imply that maintaining the culprit proteins soluble and nontoxic *in vivo* may be sufficient to allow their degradation by natural cellular clearance mechanisms, as demonstrated recently for α-synuclein.[28]

The moderate binding affinity of CLR01 for Lys residues[16] and NMR titration experiments (Supplementary Table S1) suggest that the binding is highly labile (high on−off rate). Our data support the hypothesis that this labile binding is sufficient for interfering with the weak molecular interactions that lead to

formation of oligomers or nuclei. We speculate that at the same time, the moderate-affinity binding of CLR01 may not interfere with normal cellular function until concentrations substantially higher than those needed for inhibition are used (Figure 4a). This putative mechanism needs further validation and is beyond the scope of the present study. In this context, it is important to remember that solvent-exposed Lys residues commonly are utilized for attachment of various tags (e.g., biotin, fluorescent dyes) without interfering with biological activity of stably folded proteins. It is therefore plausible that labile binding of CLR01 to these proteins would not affect their bioactivity.

Lys-specific MTs represent a novel, process-specific approach to preventing pathologic protein assembly and therefore are promising drug candidates for treatment and/or prevention of amyloid-related diseases. Recent investigation has demonstrated that CLR01 rescued Aβ-induced decrease in dendritic spine morphology and number, miniature excitatory postsynaptic currents, and long-term potentiation, and significantly reduced Aβ plaque load in the brain of AD transgenic mice.[51] These data and rescue of α-synuclein-induced toxicity in a zebrafish model[28] suggest that CLR01 also is an effective inhibitor of amyloidogenic proteins' toxicity *in vivo*.

■ ASSOCIATED CONTENT

Supporting Information. Complete refs 15 and 51, Supplementary Table S1, and Supplementary Figures S1−S9. This material is available free of charge via the Internet at http://pubs.acs.org.

■ AUTHOR INFORMATION

Corresponding Author
gbitan@mednet.ucla.edu

■ ACKNOWLEDGMENT

We thank Dr. C. Glabe, University of California, Irvine, for the A11 antibody, Dr. D. Teplow, University of California, Los Angeles, for the use of his UV spectrophotometer, fluorometer and microplate reader, and Drs. F. Rahimi, H. Li, and D. Teplow, Ms. A. Attar and Ms. T. Liu for critical suggestions and helpful discussions. This work was supported by UCLA's Jim Easton Consortium for Alzheimer's Drug Discovery and Biomarker Development (G.B.), American Health Assistance Foundation grant A2008-350 (G.B.), NIH grant RR20004 (J.A.L.), NIH/NCRR High-End Instrumentation Program S10 RR023045 (J.A.L.), NIH/NIA grant AG027818 (G.B. and G.B.B.), and by Deutsche Forschungsgemeinschaft EH100/14-1 (M.E.).

■ REFERENCES

(1) Chiti, F.; Dobson, C. M. *Annu. Rev. Biochem.* **2006**, *75*, 333–366.
(2) Greenwald, J.; Riek, R. *Structure* **2010**, *18*, 1244–1260.
(3) Gazit, E. *ACS Chem. Biol.* **2006**, *1*, 417–419.
(4) Lansbury, P. T., Jr. *Neuron* **1997**, *19*, 1151–1154.
(5) Thakur, A. K.; Jayaraman, M.; Mishra, R.; Thakur, M.; Chellgren, V. M.; Byeon, I. J.; Anjum, D. H.; Kodali, R.; Creamer, T. P.; Conway, J. F.; Gronenborn, A. M.; Wetzel, R. *Nat. Struct. Mol. Biol.* **2009**, *16*, 380–389.
(6) Nonaka, T.; Watanabe, S. T.; Iwatsubo, T.; Hasegawa, M. *J. Biol. Chem.* **2010**, *285*, 34885–34898.
(7) Marshall, K. E.; Morris, K. L.; Charlton, D.; O'Reilly, N.; Lewis, L.; Walden, H.; Serpell, L. C. *Biochemistry* **2011**, *50*, 2061–2071.
(8) Petkova, A. T.; Ishii, Y.; Balbach, J. J.; Antzutkin, O. N.; Leapman, R. D.; Delaglio, F.; Tycko, R. *Proc. Natl. Acad. Sci. U.S.A.* **2002**, *99*, 16742–16747.
(9) Usui, K.; Hulleman, J. D.; Paulsson, J. F.; Siegel, S. J.; Powers, E. T.; Kelly, J. W. *Proc. Natl. Acad. Sci. U.S.A.* **2009**, *106*, 18563–18568.
(10) Sinha, S.; Lopes, D. H. L.; Bitan, G., submitted to *Journal of Biological Chemistry* for publication, 2011.
(11) Li, W.; Sperry, J. B.; Crowe, A.; Trojanowski, J. Q.; Smith, A. B., III; Lee, V. M. *J. Neurochem.* **2009**, *110*, 1339–1351.
(12) Vana, L.; Kanaan, N. M.; Hakala, K.; Weintraub, S. T.; Binder, L. I. *Biochemistry* **2011**, *50*, 1203–1212.
(13) Cohen, T. J.; Guo, J. L.; Hurtado, D. E.; Kwong, L. K.; Mills, I. P.; Trojanowski, J. Q.; Lee, V. M. *Nat. Commun.* **2011**, *2*, 252.
(14) Huang, A.; Stultz, C. M. *PLoS Comput. Biol.* **2008**, *4*, e1000155.
(15) Winner, B.; et al. *Proc. Natl. Acad. Sci. U.S.A.* **2011**, *108*, 4194–4199.
(16) Fokkens, M.; Schrader, T.; Klärner, F. G. *J. Am. Chem. Soc.* **2005**, *127*, 14415–14421.
(17) Talbiersky, P.; Bastkowski, F.; Klärner, F. G.; Schrader, T. *J. Am. Chem. Soc.* **2008**, *130*, 9824–9828.
(18) Rahimi, F.; Maiti, P.; Bitan, G. *J. Vis. Exp.* **2009**, No. 23, No. e1071; DOI: 10.3791/1071; http://www.jove.com/index/details.stp?id=1071.
(19) Bitan, G.; Kirkitadze, M. D.; Lomakin, A.; Vollers, S. S.; Benedek, G. B.; Teplow, D. B. *Proc. Natl. Acad. Sci. U.S.A.* **2003**, *100*, 330–335.
(20) Kanapathipillai, M.; Ku, S. H.; Girigoswami, K.; Park, C. B. *Biochem. Biophys. Res. Commun.* **2008**, *365*, 808–813.
(21) Wang, S. S.; Wen, W. S. *Mol. Vision* **2010**, *16*, 2777–2790.
(22) Necula, M.; Kayed, R.; Milton, S.; Glabe, C. G. *J. Biol. Chem.* **2007**, *282*, 10311–10324.
(23) Tikhonov, A. N.; Arsenin, V. Y. *Solution of Ill-Posed Problems*; Halsted Press: Washington, DC, 1977.
(24) Xie, Y.; Zhang, J.; Yin, S.; Loo, J. A. *J. Am. Chem. Soc.* **2006**, *128*, 14432–14433.
(25) Yin, S.; Loo, J. A. *Int. J. Mass Spectrom.* **2011**, *300*, 118–122.
(26) Delaglio, F.; Grzesiek, S.; Vuister, G. W.; Zhu, G.; Pfeifer, J.; Bax, A. *J. Biomol. NMR* **1995**, *6*, 277–293.
(27) Hou, L.; Shao, H.; Zhang, Y.; Li, H.; Menon, N. K.; Neuhaus, E. B.; Brewer, J. M.; Byeon, I. J.; Ray, D. G.; Vitek, M. P.; Iwashita, T.; Makula, R. A.; Przybyla, A. B.; Zagorski, M. G. *J. Am. Chem. Soc.* **2004**, *126*, 1992–2005.
(28) Prabhudesai, S.; Sinha, S.; Kotagiri, A.; Fitzmaurice, A. G.; Klärner, F.-G.; Schrader, T.; Bitan, G.; Bronstein, J. M., submitted to *Neurotherapeutics* for publication, 2011
(29) LeVine, H., III. *Methods Enzymol.* **1999**, *309*, 274–284.
(30) Frost, B.; Ollesch, J.; Wille, H.; Diamond, M. I. *J. Biol. Chem.* **2009**, *284*, 3546–3551.
(31) Kazantzis, A.; Waldner, M.; Taylor, J. W.; Kapurniotu, A. *Eur. J. Biochem.* **2002**, *269*, 780–791.
(32) Reches, M.; Porat, Y.; Gazit, E. *J. Biol. Chem.* **2002**, *277*, 35475–35480.
(33) Andreotti, G.; Vitale, R. M.; Avidan-Shpalter, C.; Amodeo, P.; Gazit, E.; Motta, A. *J. Biol. Chem.* **2011**, *286*, 2707–2718.
(34) Frare, E.; Polverino De Laureto, P.; Zurdo, J.; Dobson, C. M.; Fontana, A. *J. Mol. Biol.* **2004**, *340*, 1153–1165.
(35) Glabe, C. G. *J. Biol. Chem.* **2008**, *283*, 29639–29643.
(36) Chimon, S.; Shaibat, M. A.; Jones, C. R.; Calero, D. C.; Aizezi, B.; Ishii, Y. *Nat. Struct. Mol. Biol.* **2007**, *14*, 1157–1164.
(37) Rahimi, A. F.; Shanmugam, A.; Bitan, G. *Curr. Alzheimer Res.* **2008**, *5*, 319–341.
(38) Kayed, R.; Head, E.; Thompson, J. L.; McIntire, T. M.; Milton, S. C.; Cotman, C. W.; Glabe, C. G. *Science* **2003**, *300*, 486–489.
(39) Lopes, D. H. J.; McDaniel, K.; Attar, A.; Klärner, F.-G.; Schrader, T.; Bitan, G. Manuscript in preparation.
(40) Alzheimer's Association; Thies, W.; Bleiler, L. *Alzheimer's Dement.* **2011**, *7*, 208−244.
(41) Rishton, G. M. *Nat. Chem. Biol.* **2008**, *4*, 159–160.

(42) Roberts, B. E.; Shorter, J. *Nat. Struct. Mol. Biol.* **2008**, *15*, 544–546.
(43) Ehrnhoefer, D. E.; Bieschke, J.; Boeddrich, A.; Herbst, M.; Masino, L.; Lurz, R.; Engemann, S.; Pastore, A.; Wanker, E. E. *Nat. Struct. Mol. Biol.* **2008**, *15*, 558–566.
(44) Yan, L. M.; Velkova, A.; Tatarek-Nossol, M.; Andreetto, E.; Kapurniotu, A. *Angew. Chem., Int. Ed.* **2007**, *46*, 1246–1252.
(45) Azriel, R.; Gazit, E. *J. Biol. Chem.* **2001**, *276*, 34156–34161.
(46) McLaurin, J.; Golomb, R.; Jurewicz, A.; Antel, J. P.; Fraser, P. E. *J. Biol. Chem.* **2000**, *275*, 18495–18502.
(47) Ladiwala, A. R.; Lin, J. C.; Bale, S. S.; Marcelino-Cruz, A. M.; Bhattacharya, M.; Dordick, J. S.; Tessier, P. M. *J. Biol. Chem.* **2010**, *285*, 24228–24237.
(48) Ladiwala, A. R.; Dordick, J. S.; Tessier, P. M. *J. Biol. Chem.* **2011**, *286*, 3209–3218.
(49) Fradinger, E. A.; Monien, B. H.; Urbanc, B.; Lomakin, A.; Tan, M.; Li, H.; Spring, S. M.; Condron, M. M.; Cruz, L.; Xie, C. W.; Benedek, G. B.; Bitan, G. *Proc. Natl. Acad. Sci. U.S.A.* **2008**, *105*, 14175–14180.
(50) Li, H.; Monien, B. H.; Lomakin, A.; Zemel, R.; Fradinger, E. A.; Tan, M.; Spring, S. M.; Urbanc, B.; Xie, C. W.; Benedek, G. B.; Bitan, G. *Biochemistry* **2010**, *49*, 6358–6364.
(51) Attar, A. et al. Manuscript in preparation.
(52) Grudzielanek, S.; Velkova, A.; Shukla, A.; Smirnovas, V.; Tatarek-Nossol, M.; Rehage, H.; Kapurniotu, A.; Winter, R. *J. Mol. Biol.* **2007**, *370*, 372–784.
(53) Teixeira, P. F.; Cerca, F.; Santos, S. D.; Saraiva, M. J. *J. Biol. Chem.* **2006**, *281*, 21998–22003.
(54) Goedert, M.; Spillantini, M. G. *Science* **2006**, *314*, 777–781.
(55) Venda, L. L.; Cragg, S. J.; Buchman, V. L.; Wade-Martins, R. *Trends Neurosci.* **2010**, *33*, 559–568.
(56) Clark, A.; Charge, S. B.; Badman, M. K.; MacArthur, D. A.; de Koning, E. J. *Biochem. Soc. Trans.* **1996**, *24*, 594–599.
(57) Melvin, K. E.; Miller, H. H.; Tashjian, A. H., Jr. *New Engl. J. Med.* **1971**, *285*, 1115–1120.
(58) Endo, J. O.; Rocken, C.; Lamb, S.; Harris, R. M.; Bowen, A. R. *J. Am. Acad. Dermatol.* **2010**, *63*, e113–114.
(59) Floege, J.; Ehlerding, G. *Nephron* **1996**, *72*, 9–26.
(60) Joao Saraiva, M.; Mendes Sousa, M.; Cardoso, I.; Fernandes, R. *J. Mol. Neurosci.* **2004**, *23*, 35–40.
(61) Plante-Bordeneuve, V.; Said, G. *Curr. Opin. Neurol.* **2000**, *13*, 569–573.
(62) Granel, B.; Valleix, S.; Serratrice, J.; Cherin, P.; Texeira, A.; Disdier, P.; Weiller, P. J.; Grateau, G. *Medicine (Baltimore, MD, U.S.)* **2006**, *85*, 66–73.
(63) Vassallo, N. *Protein Pept. Lett.* **2009**, *16*, 230–238.